IVYSPRING INTERNATIONAL PUBLISHER

Journal of Cancer

2015; 6(10): 930-937. doi: 10.7150/jca.12284

Research Paper

Transcriptomic and Functional Pathway Analysis of Human Cervical Carcinoma Cancer Cells Response to Microtubule Inhibitor

Jin Wang[1,2,✉], Bin Yan[3], Song-Mei Liu[4], Huanhuan Sun[5], Yonglong Pan[3], Daogang Guan[6], Xiaoyan Zhang[1], Jianqing Xu[1], Haiqing Ma[5,✉]

1. Scientific Research Center, Shanghai Public Health Clinical Center, 2901 Caolang Road, Jinshan District, Shanghai 201508, China
2. Department of Translational Molecular Pathology, The University of Texas, M.D. Anderson Cancer Center, Houston, TX 77030, USA
3. Laboratory for Food Safety and Environmental Technology, Institutes of Biomedicine and Biotechnology, Shenzhen Institutes of Advanced Technology, Chinese Academy of Sciences, Shenzhen 518055, China
4. Center for Gene Diagnosis, Zhongnan Hospital of Wuhan University, Wuhan, Hubei 430071, China
5. Department of Oncology, The Fifth Affiliated Hospital of Sun Yat-sen University, Zhuhai, Guangdong 519000, China
6. Department of Biology, Hong Kong Baptist University, Hong Kong, China

✉ Corresponding authors: Jin Wang, Ph.D., Scientific Research Center, Shanghai Public Health Clinical Center, 2901 Caolang Road, Jinshan District, Shanghai 201508, China; Ph: 86-21-37990333-7336; Fax: 86-21-57247094; Email: wjincityu@yahoo.com Or Haiqing Ma (haiqing_ma@163.com)

Received: 2015.03.30; Accepted: 2015.06.12; Published: 2015.07.29

Abstract

Background: There clearly is a need for effective chemotherapy for early-stage, high-risk patients with human cervical carcinoma. Vinblastine (*VBL*) is a key microtubule inhibitor, but unproven in its mechanisms as an important antitumor agent in cervical carcinoma.

Methods: We selected the concentration of vinblastine inducing 30% cell death for analyses assessing the *DNA* content, gene expression and transcriptional gene regulation of *VBL*-treated *KB-3* cells.

Results: Transcriptomic and hierarchical clustering analysis demonstrated that treatment of *KB-3* cells with *VBL* altered the expression of a diverse group of genes with *G2/M* arrest, which regulated by four oncogenic or tumor suppresser transcription factors (*AP1*, *NFKB1*, *RELA*, and *TP53*). Functional pathway analysis revealed the disease response to the biological effects of vinblastine in cervical carcinoma chemotherapy including protein ubiquitination pathway, *RhoGDI* signaling, integrin signaling, agranulocyte adhesion and biapedesis, and actin nucleation pathways. Northern blots also confirmed that *KRT-7*, *FN14*, *IER3*, and *ID1* were deregulated in *VBL*-treated *KB-3* cells.

Conclusion: Transcriptional time series profiles and a functional pathway analysis of *VBL*-treated *KB-3* cells will provide a new strategy for improving microtubule inhibitor chemotherapy for cervical carcinoma.

Key words: *KB-3* cells, vinblastine, gene expression, transcriptional gene regulation, pathway analysis.

Background

Human cervical carcinoma *KB-3* cells, representing a subclone of human HeLa cells, are highly sensitive to most chemotherapeutic drugs, clone with high efficiency, growing rapidly (1, 2). Vinblastine *(VBL)*, as a microtubule inhibitor, is an important antitumor agent that induces G_2/M arrest and subsequent apoptosis in a wide variety of cell lines (3). It was well known that *VBL* treatment caused the

down-regulation of *p53* and its target *p21* and up-regulation of tumor necrosis factor alpha and *Bak* in *KB-3* cells, identifying these genes as putative targets of vinblastine-inducible *AP-1*, which demonstrated that *VBL* -inducible *AP-1* played a destructive, proapoptotic role and regulated the expression of a specific subset of target genes (4). *p21* was also confirmed to play a protective role in *VBL*-induced apoptosis in *KB-3* cells through a c-Jun regulated pathway (5). Repression of proangiogenic and metastatic factors (*VEGF*, *bFGF*, *MMP2*, and *MMP9*) was also detected in *VBL*-treated cancer cells (6). However, the networks of affecting gene expression programs and the molecular mechanisms of antitumor of this microtubule inhibitor that link G2/M arrest and apoptosis in *VBL*-treated cervical cancer are poorly understood.

In our previous studies, 49 genes were down-regulated when *VBL*-resistant *KB-v1* cells were subjected to lower dose or depletion of *VBL* and *DNA* microarray is a very useful tool to detect drug response targets in cancer treatment (7). Thus, in view of the complex array of genetic factors contributing to *VBL* treatment of *KB-3* cells, *cDNA* microarray should be useful for examining the drug response in cancer. Identification of transcription factor (TF) target genes would help for elucidating the transcriptional control of the *VBL*-triggering gene expression programs. Thus, these analyses may ultimately enable the use of signature expression profiles of drug treatment to predict response to *VBL*, further to improve our understanding of mechanisms of microtubule inhibitor in human cervical carcinoma cancer *KB-3* cells.

Methods

Cytotoxicity assay

The sulforhodamine B (SRB) assay standard procedures were used (8). *KB-3* cells were purchased from the American Type Culture Collection and cultured in DMEM supplemented with 10% heat-inactivated fetal calf serum and the antibiotics penicillin and streptomycin. In this assay, *KB-3* cells were plated in 96-well culture plates (10^4 cells/well) and were grown overnight at 37°C in a 5% CO_2 incubator. *VBL* was then added to the wells to achieve a final concentration ranging from 10^{-6} to 10^{-4} M. Control wells were prepared by adding 100 µl culture medium. The plates were incubated at 37°C in a 5% CO_2 incubator for 48 h. After adding 50 µl of 50% trichloroacetic acid for 10 min at room temperature, the plates were then put at 4°C for 4 h and the supernatant were removed, washed 5 times with H_2O. Then, SRB was added to each well for 30 minutes. Unbound dye was removed by four washes with 1% acetic acid. The protein-bound dye was extracted with 10 mM Tris base at a wavelength of 515 nm. The LD_{50} and LD_{30} were determined from the plots of percent viability vs. dose of compound added.

Cell cycle analysis

To determine cell cycle distribution, 5 x 10^5 cell were plated in 60-mm dishes, treated with 2.5 x 10^{-4} µM of vinblastine for 0, 2, 4, 8, 12, 24, and 48 h. Cells were then collected by trypsinization, fix in 95% ethanol, wash in 1% BSA-PBS, resuspended in 1 µg/ml of RNase and 50 µg/ml of PI, incubated for 30 min in the dark at 37°C, and analyzed by flow cytometry using a FACSCalibur. The data were analyzed using the ModFit *DNA* analysis program as described previously (9).

Gene expression profiling

RNA was isolated with Trizol LS (Invitrogen, Carlsbad, CA, USA) and purified using the RNeasy Mini Kit (Qiagen, Valencia, CA, USA). RNA quality was assessed using an Agilent 2100 Bioanalyzer (Agilent Technologies, Waldbronn, DE, USA). Total RNA from each sample was labelled using a Low Input Labeling Kit (Agilent Technologies), which involves reverse transcribing the mRNA to produce cDNA and then transcribing in the presence of Cy3-CTP or Cy5-CTP to produce labelled cRNA from pancreatic cancer cell lines was paired with differentially labelled cRNA from *KB-3* cells or *VBL*-treated KB-3 cells and hybridized to a 44K Whole Human Genome Oligo Microarray (Agilent Technologies) at 60 °C for 17 h according to the manufacturer's protocol. To reduce systematic bias, dye-swap hybridizations were performed for each cell line, and the resulting data were combined with analysis, in which dye assignment was reversed in the second hybridization in Agilent arrays.

Microarray data and pathway analysis

The microarray data were represented as the antilog ratio of gene expression measures of *VBL* treated *KB-3* cells to untreated *KB-3* cells. The data were normalized and analyzed using Partek Genomics Solution software, as reported in our previous studies (10). We used the Ingenuity Pathway Analysis (IPA) tool to determine the enriched canonical pathways on the basis of differential gene expression.

Identification of transcription factor (TF) target genes

Previously, we developed a bioinformatics tool CMGRN to identify target gene of TFs and to construct gene regulatory networks, that has been successfully applied in cancer dataset (11). This method is based on Bayesian hierarchical model with Gibbs

sampling implementation to calculate joint conditional probability that genes is regulated by TFs. It is able to integrate both gene expression profiles with binding data of TFs, and to predict target genes of TFs (11). Here, we applied this methodology to integrate expression data of the differentially expressed genes (fold change at least 1.5) from the *VBL*-treated microarray experiment and the binding data of four TFs, *NFKB1*, *RELA*, *AP1* and *TP53* derived from Yan et al (12). As a result, we will predict target genes of the four TFs and then infer the transcriptional gene regulatory networks.

Northern blotting

Total cellular *RNA* of untreated or *VBL*-treated *KB-3* cells was isolated as described previously (7), run on a 1% agarose gel (15 g per gel lane) containing 2.2 M formaldehyde, and transferred to a nitrocellulose membrane. Membrane was dried at room temperature, and *RNA* was cross-linked by UV irradiation in a Stratalinker (Stratagene). Hybridization was performed in ExpressHyb Hybridization buffer (CLONTECH) containing 1 x 10^6 cpm/ml of ^{32}P-labeled *cDNA* probe (*ID1, IER3, KRT-7, FN14* and *β-actin*) at 65°C for 2 h. Blots were washed in 2 x SSC and 0.1% SDS for 20 min, followed by a wash at 50°C in 0.2 x SSC and 0.1% SDS for 20 min.

Results

Flow cytometry analysis of the effect of vinblastine on *KB-3* cells.

First, we tested the cytotoxicity of vinblastine in human cervical carcinoma *KB-3* cells using Sulforhodamine B (SRB) assay as described previously (8). After *KB-3* cells were treated with *VBL* for 48 h, the median lethal dose (LD_{50}) and the concentration of vinblastine at which 30% cell death was reached (LD_{30}) in *KB-3* cells were 6.8 x 10^{-4} μM and 2.5 x 10^{-4} μM, respectively. The flow cytometry assay provides information regarding cell cycle phase sensitivity to apoptosis is based on bivariate analysis of their DNA content (9). Next, the concentration of LD_{30} was selected for analyses assessing the DNA content of vinblastine-treated *KB-3* cells, which was examined via propidium iodide (PI) staining and flow cytometry. At 0, 2, 4, 8, 12, 24, and 48 h post-treatment with 2.5 x 10^{-4} μM of vinblastine, *KB-3* cells arrested predominately at *G2/M* phase of the cell cycle and the number of cells in the *G1* phase had diminished (Fig. 1). With a longer duration of treatment (24 h), a much greater percentage of *KB-3* cells at *G2/M* phase. These results indicate that *KB-3* arrested at *G2/M* in response to vinblastine treatment.

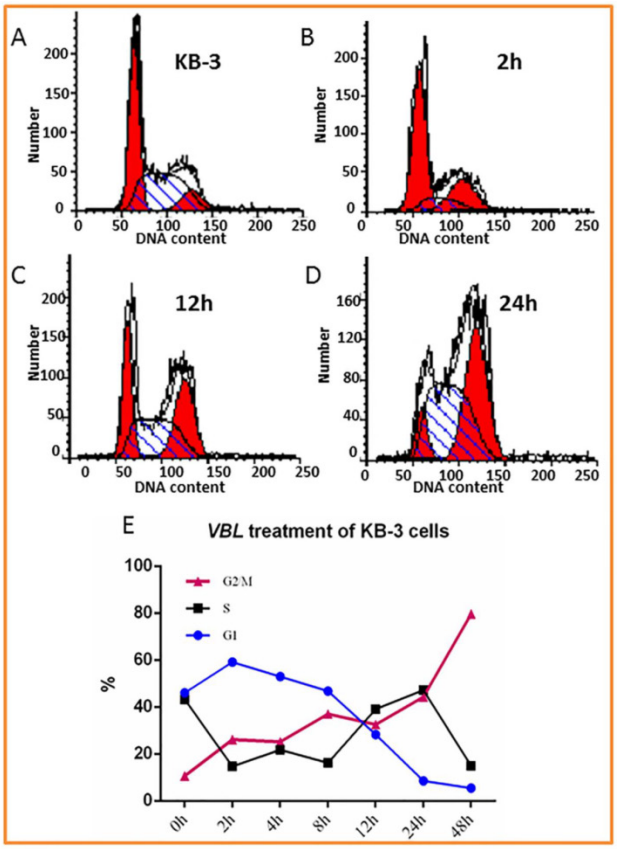

Figure 1. Effect of vinblastine (*VBL*) on cellular DNA content. *KB-3* cells untreated and treated with 2.5 x 10^{-4} μM of vinblastine for 2, 4, 8, 12, 24, and 48 h. Cells were subjected to DNA content analysis by flow cytometry with PI staining. A-D: *KB-3* cells treated with 2.5 x 10^{-4} μM of *VBL* for 0, 2, 12 and 24h. E: Data analysis of Effect of *VBL* on cellular DNA content in *KB-3* cells treated with 2.5 x 10^{-4} μM of *VBL* for 0, 2, 4, 8, 12, 24, and 48 h.

Gene clustering analysis showing the differentially expressed genes in *VBL* treated *KB-3* cells in a time-dependent manner.

The *VBL* response gene candidates were selected based on the patterns from a heat-map figure (Fig. 2) from the 73 normalized gene lists via Partek Genomic Suite. The red is for the up-regulated genes, blue is for down-regulated genes, white is for the missing data in a time point, which were from differently expressed genes in *KB-3* cells treated with 2.5 x 10^{-4} μM of vinblastine at 0, 2, 4, 8, 12, 16, 24, and 48 h, and identified to change in the transcriptome at a normal cutoff value ≥ ± 1.5-fold in 80% tested samples. Hierarchical clustering has the advantage that it is simple and the results can be easily visualized (13), and was used to partition data into two groups that have similar expression patterns (Fig. 2). These classes of genes could be distinguished into those whose *m*RNA levels remained induced for much longer (Fig. 2, cluster A) and those that responded early and whose induction was transient (Fig 2. cluster B), which included *IER3, SCO2, SP140, ID1, DUSP6, ADRM1, U2AF1, NUDEL, SLC26A6, BCAA, PPID, SKD1, SPHK1*, and *SGK*.

Over-expressed genes in *MDR KB-v1* cells can also be found in cluster A, which showed gradually increasing gene expression in *VBL* treatment of *KB-3* cells as a function of time, including the genes that responded later (*KRT 7, KRT 17, FN14, UGT2B7, ITGA5*, and *CD63*) that appeared to be related to drug resistance involving cell wall metabolism, drug modification, and signal transduction (7). The transcriptional response to vinblastine suggests a multifaceted role for *KB-3* cells in the physiology of drug metabolism.

Northern blot analysis was used to verify the array hybridization data.

Northern blot analysis of *ID1, IER3, KRT-7, FN14,* and β-actin was performed on *RNA* prepared from *KB-3* cells that were treated with 2.5 x 10^{-4} μM *VBL* for 0, 2, 4, 8, 12, 16, and 24 h and demonstrated that *ID1, IER3, KRT-7*, and *FN14* were deregulated in *KB-3* cells treated with *VBL* compared to *β-actin* as control (Fig. 3). Northern blot analysis of deregulated genes in *KB-3* cells treated with *VBL* verified the array hybridization data.

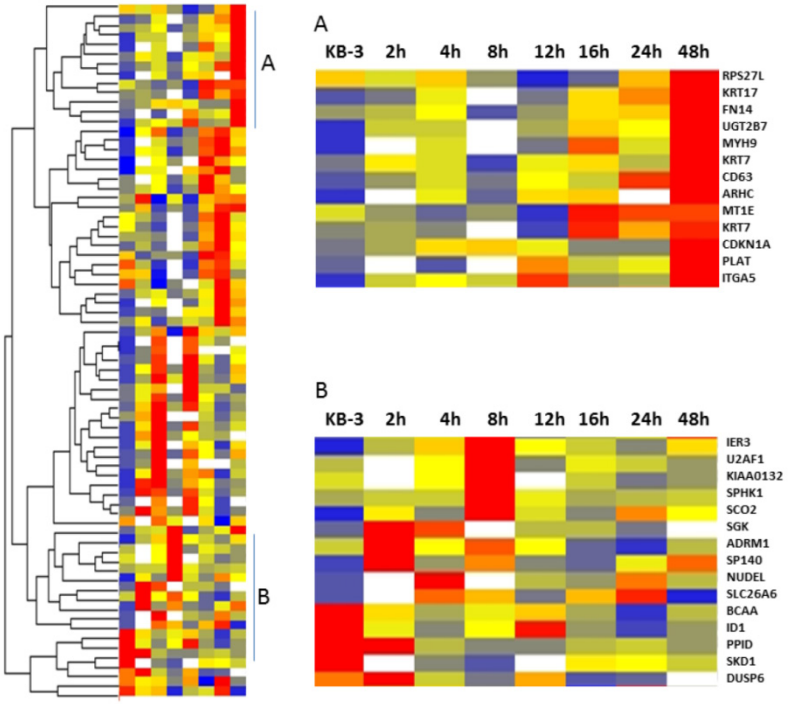

Figure 2. Cluster image showing the different classes of gene expression profiles. Five hundred thirty-six genes whose RNA levels changes in response to 2.5 x 10^{-4} μM of vinblastine were selected. This subset of genes was clustered hierarchically into groups on the basis of the similarity of their expression profiles. The graphs show the average expression profiles for the genes in the corresponding cluster A and B.

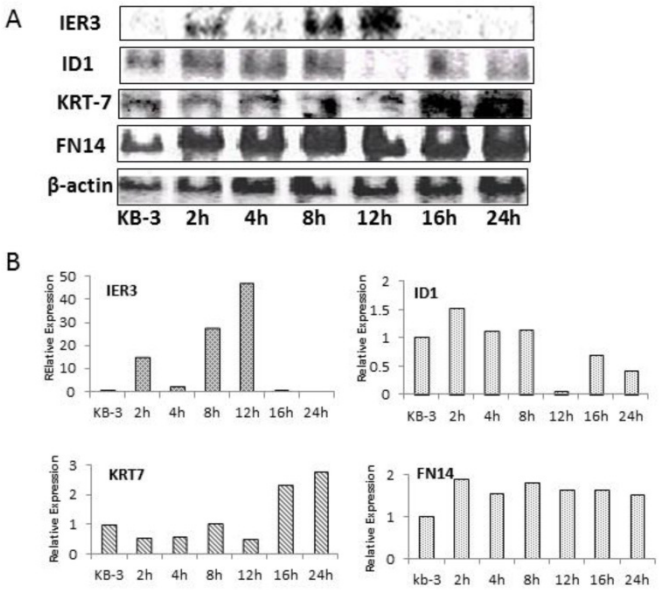

Figure 3. Northern Blots analysis of *ID1*, *IER3*, *KRT-7* and *FN14*, and *ß-actin* was used to normalize the RNA quantity in each sample (A). Analyzed the quantification of the mRNA expression levels of *ID1*, *IER3*, *KRT-7* and *FN14* those normalized to *ß-actin* in *KB-3* cells treated with vinblatine (B).

Functional networks and pathways of *VBL*-induced stress response in human cervical carcinoma *KB-3* cells were analyzed by the Ingenuity Pathway Analysis (IPA).

The genetic networks and cellular pathways were derived using the IPA program by analyzing 73 genes that were differentially expressed in *VBL*-treated *KB-3* cells. A more comprehensive network and pathway analysis of all deregulated genes revealed their association with four important network functions and five critical canonical pathways, all of which are relevant to *VBL*-treated *KB-3* cells. The differently expressed genes constituted about half the total molecules involved and the network-associated cellular functions and included those related to dermatological diseases and conditions, inflammatory disease, inflammatory response, energy production, cellular development, digestive system development and function, embryonic development, organ development, cancer, and cellular movement in *VBL*-treatment of cells (Table 1). They belong to five canonical signaling pathways that are commonly deregulated in *VBL* treatment (Table 2). Although only 14 (*HSPA8, PSMD11, PSMC1, HLA-C, PSMD1, PSMD8, RHOC, ITGA5, RHOF, ACTG1, MSN, MYH9, CLDN1*, and *CAPN2*) were deregulated in *VBL*-treated *KB-3* cells with the protein ubiquitination, *RhoGDI* signaling, integrin signaling, agranulocyte adhesion and biapedesis, and actin nucleation signaling pathways, which play a role in in controlling cancer cell growth, microtubule inhibition, and the stress response of *VBL*- treated *KB-3* cells.

Transcriptional gene regulatory network in *VBL*-treated cells

It has been demonstrated that some oncogenic or tumor suppresser TFs are implicated in affecting gene expression programs in cervical cancer, such as *NF-κB* (14, 15), *AP1* (4, 14), and *TP53* (16). In order to elucidate how these cancer-related TFs affect the response of *VBL*-treated *KB-3* cells, we employed a newly developed bioinformatics method to identify their target genes (11). As shown in Table 3, we display the predicted target genes of *AP1*, *NFKB1*, *RELA*, and *TP53*. Some target genes have been validated in previous studies, for example, *CDKN1A (p21), DUSP5, IER3, ITGA5*, *RPS27L* and *SOD2* (Table 3). We constructed a transcriptional gene regulatory network controlled by the four TFs (Fig. 4). Noticed is that nine genes are co-targeted by oncogenic (*AP1*, *NFKB1* and *RELA*) and tumor suppresser TFs (*TP53*), and involve biological processes apoptosis (*CDKN1A* and *SPHK1*), calcium-activated neutral proteinase (*CAPN2*), epidermis development (*EMP1, ACTG1, KRT14, KRT15* and *KRT17*), and tumor-associated antigen (*MAGED2*). By contrast, the oncogenic TFs also regulate genes related with ubiquitin-protein modification (*PSMD11* and *PSMD1*), apoptosis (*IEG3*), and cell adhesion (*ITGA5* and *MSN*). This result indicates a possibility of transcriptional gene regulation that mediates the *VBL*-induced response in the cancer cells.

Table 1. Genetic networks associated with *VBL*-treated *KB-3* cells.

Top 4 VBL networks	Score	Focus molecules	Molecules in network
Dermatological diseases and conditions, inflammatory disease, inflammatory response	42	19	19S proteasome, 20s proteasome, 26s Proteasome, Actin, **ADRM1**, Alpha tubulin, ATPase, **CD63**, Cytokeratin, ENaC, ERK1/2, **ID1, IER3, KRT7, KRT14, KRT15, KRT17**, Mlc, **MYH9**, Myosin, **POLK**, PP2A, **PSMC1**, PSMD, **PSMD1**, **PSMD8, PSMD11, RACGAP1, RHOC**, Rock, Smad, **SMAD2**, Ubiquitin, **VPS4B, WNK1**
Energy production, cellular development, digestive system development and function	31	15	**ABCF1, ANXA3**, ATG4D, C1orf50, Calmodulin, **DDX5**, ERK, FAM216A, **FBXO9**, GDAP2, **HLA-C**, HNF1A, HNF4A, **LOC102724594/U2AF1**, **MRPL19, MRPL33**, MTRF1L, ORMDL2, **PAM**, Pka, **PLP2, PRMT3**, RNF44, SLC35D1, SLC7A6OS, SNX11, **SP140, TAGLN2**, TMUB2, **TPM4**, UBC, **UGT2B7**, ZNF155, ZNF442, ZNF586
Embryonic development, organ development,	28	14	**ACTG1, AKR1B1**, Alpha catenin, **ANXA4**, caspase, CD3, **CDKN1A**, Clathrin, cytochrome C, estrogen receptor, F Actin, Hdac, Histone h3, Histone h4, **HSPA8**, IL12 (complex), Insulin, Interferon alpha, Jnk, **LGALS3BP**, **MAGED2, MBD1, MSN**, NFkB (complex), Notch, P38 MAPK, PI3K (complex), **PPID**, Pro-inflammatory Cytokine, Ras homolog, **RHOF**, RNA polymerase II, **RPS3, RPS27L, SGK1**
Cancer, cellular movement	23	12	Akt, Alp, Ap1, **AURKA**, calpain, **CAPN2**, Cg, **CLDN1**, Creb, Cyclin A, **DUSP5**, Fibrinogen, Focal adhesion kinase, FSH, IL1, **ITGA5**, LDL, Lh, Mek, **MT1E, MT1L**, NMDA Receptor, **NT5E**, p85 (pik3r), Pdgf (complex), PDGF BB, Pkc(s), **PLAT**, PLC gamma, Ras, **SLC26A6, SOD2, SPHK1**, Tgf beta, VegfF

Table 2. Top 5 canonical pathways involving genes that are differently expressed in *VBL*- treated *KB-3* cells, as determined by Ingenuity Pathway Analysis.

Top 5 Canonical Pathways	P value	Ratio	Molecules
Protein Ubiquitination Pathway	1.31E-04	2.35E-02	HSPA8, PSMD11, PSMC1, HLA-C, PSMD1, PSMD8
RhoGDI Signaling	1.91E-04	2.89E-02	RHOC, ITGA5, RHOF, ACTG1, MSN
Agranulocyte Adhesion and Diapedesis	2.88E-04	2.65E-02	MYH9, CLDN1, ITGA5, ACTG1, MSN
Integrin Signaling	3.90E-04	2.48E-02	RHOC, ITGA5, CAPN2, RHOF, ACTG1
Actin Nucleation	6.84E-04	5.36E-02	RHOC, ITGA5, RHOF

Table 3. Transcription factor target genes in *VBL*-treated tumor cells.

Gene symbol	AP1	NFKB1	RELA	TP53
ACTG1		predicted target		predicted target
AKR1B1		predicted target	predicted target	
CAPN2	predicted target	predicted target		predicted target
CD63	predicted target	predicted target		
CDKN1A	***validated target***	***validated target***	***validated target***	***validated target***
CLDN1		predicted target		
DUSP5				***validated target***
EMP1	predicted target			predicted target
HLA-C		predicted target		
HSPA8		predicted target		
IER3		***validated target***	***validated target***	
ITGA5	predicted target	***validated target***	***validated target***	
KCNK1		predicted target		
KRT14	predicted target			predicted target
KRT15			predicted target	predicted target
KRT17		predicted target		predicted target
LASP1		predicted target		
LGALS3BP				predicted target
MAGED2	predicted target	predicted target		predicted target
MORF4L2	predicted target			
MSN		predicted target	predicted target	
MT1E		predicted target		
MYH9		predicted target		
MYO1C	predicted target			
PAM	predicted target	predicted target		
PLP2	predicted target	predicted target	predicted target	
PSMC1	predicted target			
PSMD1	predicted target	predicted target		
PSMD11	predicted target	predicted target		
PSMD8				predicted target
RAB31	predicted target	predicted target	predicted target	
RPS27L				***validated target***
SDC4		predicted target	predicted target	
SOD2				***validated target***
SPHK1	predicted target	predicted target		predicted target
STC2			predicted target	
TAGLN2		predicted target		
TPM4		predicted target		

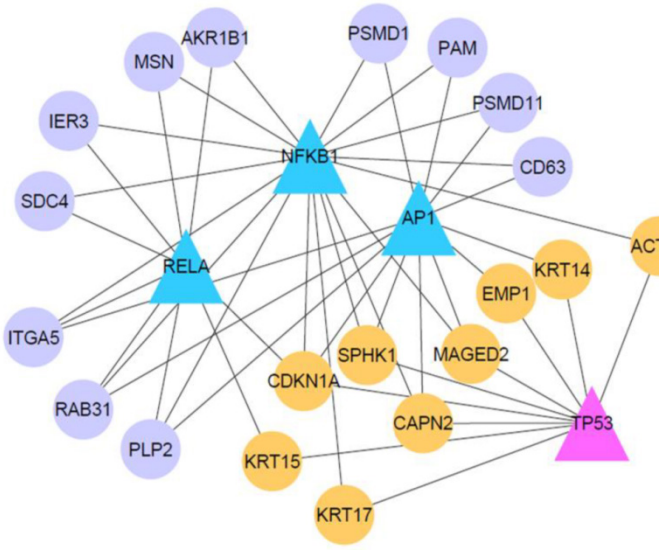

Figure 4. Transcriptional gene regulatory network in *VBL*-treated *KB-3* cell. Triangle nodes represent four TFs *AP1*, *NFKB1*, *RELA* and *TP53*. Circle nodes refer to target genes of at least two TFs. Orange nodes refer to genes jointly regulated by TP53 and other TFs.

Discussion

In this study, first, cytotoxicity studies and the flow cytometry assay provided information regarding the cytotoxicity of microtubule inhibitor in *KB-3* cells and cell cycle phase sensitivity to apoptosis is based on bivariate analysis of their *DNA* content. The *DNA* content of untreated and *VBL*-treated *KB-3* cells was examined via PI staining and flow cytometry. At 12 h post-treatment with 2.5 x 10^{-4} µM of *VBL* (LD_{30}), *KB-3* cells were arrested predominately at *G2/M* phase of the cell cycle and *G1* phase was apparently decreased (Fig. 1). Under a longer duration of treatment, a much greater percentage of *KB-3* was arrested at *G2/M* phase. The result indicated that *KB-3* arrested at *G2/M* in response to *VBL*. At the same time, the hierarchical clustering analysis revealed that *RPS27L, KRT17, FN14, UGT2B7, MYH9, CD63, ARHC, MT1E, KRT7, CDKN1A, PLAT*, and *ITGA5* were responsible for *KB-3* cells arrested predominately at *G2/M* phase of the cell cycle with 2.5 x 10^{-4} µM vinblastine, which were highly overexpressed in *VBL*-treated *KB-3* cells that responded later including those that control the cell

cycle, *DNA* repair, and drug resistance. In these later response genes, *RPS27L*-expressing *LoVo* cells ceased *DNA* synthesis and apoptotic activity, and elevated *RPS27L* may improve the prognoses of certain CRC patients by enhancing the *DNA* repair capacity of their colonic cells (17). *CDKN1A*, as a negative regulator of cell proliferation and *DNA* replication, plays additional and fundamental roles in other important pathways, including regulation of transcription, apoptosis and *DNA* repair (18). *UGT2B7* is an enzyme responsible for detoxification of xenobiotics, as one of the most active UDP-glucuronosyltransferases, involved in drug metabolism and in maintaining homeostasis of endogenous compounds (19). The expression of keratins is highly dependent on the state of cell development and differentiation and varies within different types of epithelia (20-22). For example, the incidence of a positive expression for *KRT7* and *KRT17* was significantly higher in desmoplastic malignant mesothelioma than in fibrous pleuritis (23). Fibroblast growth factor-inducible 14 (*FN14*) protein expression was associated with the invasive and metastatic potential of *NSCLC* and promotes hepatocyte growth factor receptor (*HGFR/MET*)-driven cell invasion (24). Our Northern blot validation of gene expression profiles confirmed that *KRT-7* and *FN14* were upregulated genes that responded later in *KB-3* cells.

On the other hand, Figure 2 also shows that Cluster B of genes in the transcriptional program of *KB-3* cells in early response to vinblastine treatment share similar expression patterns in transcript levels, which *m*RNA levels increase at 2, 4, and 8 h with vinblastine treatment, includes *IER3, ID1, SCO2, SP140, DUSP6, ADRM1, U2AF1, NUDEL, SLC26A6, BCAA, PPID, SKD1, SPHK1*, and *SGK*, which are known or likely to be involved in stress response, apoptosis, and PI3K/Akt signal transduction pathways. *IER3* (early response gene immediate early response 3), which is induced by various stimuli, such as growth factors, cytokines, ionizing radiation, viral infection, and other types of cellular stress, plays a complex and to some extent contradictory role in cell cycle control and apoptosis (25). The lack of *IER3* expression is associated with a deregulation of the *NF-κB* and *PI3K/Akt* pathways (26, 27), which represents a novel mechanism of *Nrf2* regulation that may be lost in tumors and by which *IER3* exerts its stress-adaptive and tumor-suppressive activity (28). Additionally, inhibitor of *DNA* binding (*ID*) family members are key regulatory proteins in a wide range of developmental and cellular processes and function by inhibiting target proteins that include the basic helix-loop-helix transcription factors (29). *ID1* and *ID3* function together to govern colon cancer-initiating cell self-renewal through *p21* driven cell-cycle restriction (30). Based on the bioinformatics model analysis, we demonstrated that four major TFs (*AP1*, *NFKB1*, *RELA*, and *TP53*) and the downstream genes likely form regulatory networks to modulate genes expression programs related with the *VBL*-induced response in cervical cancer cells. Two members of *NF-κB*, *RELA* and *NFKB1*, can regulate *IER3* and *p21*, providing evidence for involvement of this oncogenic TF in response of *KB-3* cells to *VBL* through targeting apoptosis signaling. Our Northern blot analyses further confirmed that *IER3* and *ID1* were upregulated genes those responded early in *KB-3* cells.

Last, we demonstrated that 14 genes, deregulated in *VBL*-treated *KB-3* cells, were involved in five signaling pathways including protein ubiquitination pathway (*HSPA8, PSMD11, PSMC1, HLA-C, PSMD1, PSMD8*), *RhoGDI* signaling (*RHOC, ITGA5, RHOF, ACTG1* and *MSN*), agranulocyte adhesion and biapedesis (*MYH9, CLDN1, ITGA5, ACTG1* and *MSN*), integrin signaling (*RHOC, ITGA5, CAPN2, RHOF* and *ACTG10*), and actin nucleation by *ARP-WASP* complex (*RHOC, ITGA5, RHOF*) (Table 2). Gene network analysis reveals that cancer-related TFs are able to regulate these pathway genes, such as *PSMD1, PSMD11, ITGA5* and *MSN* (Fig. 4). These functional pathways will help us understand the response of human cervical carcinoma to the biological effects of microtubule inhibitor as chemotherapy.

In summary, the present results represent an important advancement and provide a sound basis for further exploration, but we also recognize that *in vitro* results almost certainly represent a distorted and incomplete rendering of the normal physiological response of *KB-3* cells to microtubule inhibitor. Transcriptional profiles and pathway analysis offer an opportunity to generate functional data on a genome-wide scale. Thus, mediating protein ubiquitination, *RhoGDI* signaling, and integrin signaling pathways may have a direct and effective impact on human cervical carcinoma treatment with microtubule inhibitor.

Abbreviations

CAPN2, Calcium-activated neutral proteinase; FN14, Fibroblast growth factor-inducible 14; IER3, Early response gene immediate early response 3; IPA, Ingenuity pathway analysis; ID, Inhibitor of DNA binding; LD_{50}, Median lethal dose; SRB, Sulforhodamine B; TF, Transcription factor; VBL, Vinblastine.

Conflict of Interest

All authors have no conflict of interest.

Acknowledgment

The work described in this paper was supported by National Natural Science Foundation of China Grants 81271919 and 81072496H1014, and the work in Jin Wang's laboratory is supported partially by a grant (RCJJP21) from Shanghai Public Health Clinical Center, China.

References

1. Nelson-Rees WA, Flandermeyer RR. HeLa cultures defined. Science. 1976, 191(4222):96-98.
2. Yue B, Zhao CR, Xu HM, et al. Riccardin D-26, a synthesized macrocyclic bisbibenzyl compound, inhibits human oral squamous carcinoma cells KB and KB/VCR: In vitro and in vivo studies. Biochim Biophys Acta. 2013, 1830(1):2194-2203.
3. Studzinski GP, Bhandal AK, Brelvi ZS. Cell cycle sensitivity of HL-60 cells to the differentiation-inducing effects of 1-alpha,25-dihydroxyvitamin D3. Cancer Res. 1985, 45(8):3898-3905.
4. Fan M, Goodwin ME, Birrer MJ, et al. The c-Jun NH(2)-terminal protein kinase/AP-1 pathway is required for efficient apoptosis induced by vinblastine. Cancer Res. 2001, 61(11):4450-4458.
5. Bene A, Chambers TC. p21 functions in a post-mitotic block checkpoint in the apoptotic response to vinblastine. Biochem Biophys Res Commun. 2009, 380(2):211-217.
6. Auyeung KK, Law PC, Ko JK. Combined therapeutic effects of vinblastine and astragalus saponins in human colon cancer cells and tumor xenograft via inhibition of tumor growth and proangiogenic factors. Nutr Cancer. 2014, 66(4):662-674.
7. Wang J, Tai LS, Tzang CH, et al. 1p31, 7q21 and 18q21 chromosomal aberrations and candidate genes in acquired vinblastine resistance of human cervical carcinoma KB cells. Oncol Rep. 2008, 19(5):1155-1164.
8. Skehan P, Storeng R, Scudiero D, et al. New colorimetric cytotoxicity assay for anticancer-drug screening. J Natl Cancer Inst. 1990, 82(13):1107-1112.
9. Wang J, Fong CC, Tzang CH, et al. Gene expression analysis of human promyelocytic leukemia HL-60 cell differentiation and cytotoxicity induced by natural and synthetic retinoids. Life Sci. 2009, 84(17-18):576-583.
10. Wang J, Chan JY, Fong CC, et al. Transcriptional analysis of doxorubicin-induced cytotoxicity and resistance in human hepatocellular carcinoma cell lines. Liver Int. 2009, 29(9):1338-1347.
11. Guan D, Shao J, Deng Y, et al. CMGRN: a web server for constructing multi-level gene regulatory networks using ChIP-seq and gene expression data. Bioinformatics. 2014, 30(8):1190-1192.
12. Yan B, Li H, Yang X, et al. Unraveling regulatory programs for NF-kappaB, p53 and microRNAs in head and neck squamous cell carcinoma. PLoS One. 2013, 8(9):e73656.
13. Iyer VR, Eisen MB, Ross DT, et al. The transcriptional program in the response of human fibroblasts to serum. Science. 1999, 283(5398):83-87.
14. Kim SH, Oh JM, No JH, et al. Involvement of NF-kappaB and AP-1 in COX-2 upregulation by human papillomavirus 16 E5 oncoprotein. Carcinogenesis. 2009, 30(5):753-757.
15. Song LL, Peng Y, Yun J, et al. Notch-1 associates with IKKalpha and regulates IKK activity in cervical cancer cells. Oncogene. 2008, 27(44):5833-5844.
16. Ojesina AI, Lichtenstein L, Freeman SS, et al. Landscape of genomic alterations in cervical carcinomas. Nature. 2014, 506(7488):371-375.
17. Huang CJ, Yang SH, Lee CL, et al. Ribosomal protein S27-like in colorectal cancer: a candidate for predicting prognoses. PLoS One. 2013, 8(6):e67043.
18. Stivala LA, Cazzalini O, Prosperi E. The cyclin-dependent kinase inhibitor p21CDKN1A as a target of anti-cancer drugs. Curr Cancer Drug Targets. 2012, 12(2):85-96.
19. Menard V, Collin P, Margaillan G, et al. Modulation of the UGT2B7 enzyme activity by C-terminally truncated proteins derived from alternative splicing. Drug Metab Dispos. 2013, 41(12):2197-2205.
20. Coulombe PA, Lee CH. Defining keratin protein function in skin epithelia: epidermolysis bullosa simplex and its aftermath. J Invest Dermatol. 2012, 132(3 Pt 2):763-775.
21. Moll R, Divo M, Langbein L. The human keratins: biology and pathology. Histochem Cell Biol. 2008, 129(6):705-733.
22. Simpson CL, Patel DM, Green KJ. Deconstructing the skin: cytoarchitectural determinants of epidermal morphogenesis. Nat Rev Mol Cell Biol. 2011, 12(9):565-580.
23. Horiuchi T, Ogata S, Tominaga S, et al. Immunohistochemistry of cytokeratins 7, 8, 17, 18, and 19, and GLUT-1 aids differentiation of desmoplastic malignant mesothelioma from fibrous pleuritis. Histol Histopathol. 2013, 28(5):663-670.
24. Whitsett TG, Fortin Ensign SP, Dhruv HD, et al. FN14 expression correlates with MET in NSCLC and promotes MET-driven cell invasion. Clin Exp Metastasis. 2014, 31(6):613-623.
25. Arlt A, Schafer H. Role of the immediate early response 3 (IER3) gene in cellular stress response, inflammation and tumorigenesis. Eur J Cell Biol. 2011, 90(6-7):545-552.
26. Arlt A, Kruse ML, Breitenbroich M, et al. The early response gene IEX-1 attenuates NF-kappaB activation in 293 cells, a possible counter-regulatory process leading to enhanced cell death. Oncogene. 2003, 22(21):3343-3351.
27. Osawa Y, Nagaki M, Banno Y, et al. Expression of the NF-kappa B target gene X-ray-inducible immediate early response factor-1 short enhances TNF-alpha-induced hepatocyte apoptosis by inhibiting Akt activation. J Immunol. 2003, 170(8):4053-4060.
28. Stachel I, Geismann C, Aden K, et al. Modulation of nuclear factor E2-related factor-2 (Nrf2) activation by the stress response gene immediate early response-3 (IER3) in colonic epithelial cells: a novel mechanism of cellular adaption to inflammatory stress. J Biol Chem. 2014, 289(4):1917-1929.
29. Perk J, Iavarone A, Benezra R. Id family of helix-loop-helix proteins in cancer. Nat Rev Cancer. 2005, 5(8):603-614.
30. O'Brien CA, Kreso A, Ryan P, et al. ID1 and ID3 regulate the self-renewal capacity of human colon cancer-initiating cells through p21. Cancer Cell. 2012, 21(6):777-792.